Curcumin Resuscitate Gliadin Induced Oxidative Damage And Altered Cellular Responses In Human Intestinal Cells Via Cross-Talk Between The Transcription Factor Nrf-2 And Multifunctional Protein APE1

Kunj Bihari Gupta
Central University of Punjab
Anil Kumar Mantha
Central University of Punjab
Monisha Dhiman (monisha.dhiman@cup.edu.in)
Central University of Punjab https://orcid.org/0000-0001-5923-3384

Research Article

Keywords: Gliadin protein, Wheat allergies, Curcumin, Oxidative stress, Antioxidant response, Nrf-2, APE1

Posted Date: June 24th, 2021

DOI: https://doi.org/10.21203/rs.3.rs-614185/v1

Abstract

An imbalance between the production of oxygen and nitrogen free radicals and their degradation by the antioxidant system are the major causative factors for the wheat intolerance diseases. In the present study, we have examined the wheat gliadin protein-induced oxidative and nitrosative stress and downstream responses in the human intestinal cell lines viz. HCT-116 and HT-29. The role of phytochemical curcumin was investigated to alleviate the gliadin associated cellular damages. The focus of the study was to identify the role of key DNA repair enzyme apurinic/apyrimidinic endonuclease 1 (APE1) in gliadin protein-induced toxicity in the intestine, which may be crucial for establishing the gut-associated diseases. Reactive oxygen species (ROS); reactive nitrogen species (RNS); mitochondrial ROS; mitochondrial trans-membrane potential; protein carbonylation; lipid peroxidation; and the oxidized DNA base damage was estimated in HCT-116 and HT-29 cells after 24 h treatment of 160 µg/ml of gliadin, 10 µM of curcumin and its combination. In addition, the transcriptional expression and enzymatic activities of antioxidants (SOD; Catalase; and GSH) were measured in the in these cells. Furthermore, the cross-talk between the nuclear factor erythroid 2-related factor-2 (Nrf-2) and the multifunctional enzyme APE1 was analyzed by the immunofluorescent based imaging and co-immunoprecipitation assays. The endonuclease activity of APE1 and the DNA-protein interaction of NRF-2 with ARE was analyzed by using electrophoretic mobility shift assay (EMSA) with the nuclear lysates of HCT-116 and HT-29 cells. Results suggest that 3 h pre-treatment of curcumin followed by the treatment of gliadin protein for 24 h time protect the HCT-116 and HT-29 cells via (1) decreasing the ROS, RNS, oxidative stress, mitochondrial ROS, recuperate mitochondrial trans-membrane potential; (2) reestablishing the cellular antioxidant defence systems; (3) enhancing the DNA-repair via APE1 and which further activates the ARE elements via activation of Nrf-2. In conclusion, wheat gliadin induces the oxidative/nitrosative stress, mitochondrial damage and damages the cellular biomolecules; hence is associated with the disease pathogenesis and tissue damage in wheat intolerance diseases. The gliadin induced stress and its consequences are significantly reduced by the pre-treatment of curcumin via DNA repair pathways and oxidative stress which is evident through the interaction between two essential proteins of these pathways APE1 and Nrf-2 hence suggesting the role of curcumin based management of wheat intolerance diseases like celiac disease.

Introduction

Wheat is a staple food of many countries, including India and provides about 20% of calories intake from the total food consumption. It is an important source of dietary proteins, carbohydrates and other essential nutritional components. Despite their plenty of benefits, wheat proteins are the main cause of many diet-induced health issues like wheat protein-induced allergies, Celiac disease (CD), Non-celiac gluten sensitivity (NCGS), wheat intolerance etc. Wheat grain proteins are of two types, either metabolic proteins or storage proteins. Metabolic proteins are albumin and globulin; whereas storage protein is gluten which includes gliadin and glutenin. These storage proteins are responsible for the unique viscoelastic characteristics of wheat dough and provide rheological properties to the wheat flour, which is

essential for food processing and bakery (Liu et al. 2010). The stored proteins are the main trigger for different allergic reactions and can induce autoimmune responses in genetically susceptible individuals. In the recent years, the prevalence of wheat-related allergies have drastically increased in the general population, where the prevalence of CD is about 1% worldwide (Singh et al. 2018), NCGS is about 0.5–13% (Molina-Infante et al. 2015), and other wheat allergies/hypersensitivity is about 0.1% – 3.6% (Scherf 2019). The key players of these diseases are the excessive production of ROS/RNS, oxidative stress, and imbalance in the antioxidant defence system (Monguzzi et al. 2019; Moretti et al. 2018). Oxidative stress due to deficiencies in cellular repair processes or change in mitochondrial redox potentials can result in persistently high levels of oxidative base lesions in the DNA. APE1, a primary enzyme responsible for recognition and incision of apurinic/apyrimidinic/abasic (AP) sites in the DNA; and is also responsible for the redox activation of multiple cellular transcription factors (TFs) like nuclear factor-kappa B (NF-κB), activator protein 1 (AP-1), hypoxia-inducible factor 1-alpha (HIF-1α), Nrf-2 etc. (Thakur et al. 2015). Nrf-2, a redox-sensitive transcription factor and the master regulator of phase-II antioxidant enzymes; controls the expression of a range of antioxidant response element (ARE) dependent genes to regulate the physiological and pathological consequences (Sun et al. 2007). There are many phytochemicals with antioxidant properties out of which one of the most common is curcumin; a most studied and primary active curcuminoid of turmeric which is derived from the rhizome of *Curcuma longa* (Amalraj et al. 2017). Curcumin scavenges the endogenous ROS and RNS by modulating the Nrf-2, NF-κB, and AP-1 proteins (González-Reyes et al. 2013; Pinkus et al. 1996). In the present study, we have examined the gliadin (a main storage protein of the wheat grain) induced oxidative and nitrosative stress and its consequences in the human colon cancer cell lines HCT-116 and HT-29. The role of phytochemical curcumin to modulate the harmful effects of gliadin via functional interaction between APE1 and Nrf-2 are studied, advocating for the functional role, and the cross-talk between these two critical cellular bio-molecules is essential for therapeutic interventions for the human wheat allergies.

Materials And Methods

Cell culture

Human colon cancer cell lines HCT-116 and HT-29 were purchased from the National Centre for Cell Sciences (NCCS), Pune, India. Both the cell lines were cultured in high glucose Dulbecco's Modified Eagle's Minimal Essential Medium (DMEM; Gibco/ HyClone) supplemented with 10% heat-inactivated FBS (Gibco/ Sigma-Aldrich), 1X antibiotic solution (penicillin-streptomycin; HiMedia) in tissue culture flasks (Corning) at 37°C in a humidified atmosphere of 5% CO_2 incubator (New Brunswick, Galaxy® 170S). The 70 to 80% confluent cells were trypsinized using 1X trypsin-EDTA and sub-cultured for further experiments (Gupta et al. 2018).

Treatment of cells

The HCT-116 and HT-29 cells were seeded in 60mm/100mm culture dishes at a cell density $1\times10^5/1\times10^6$ per plate. Overnight cultured cells were treated with gliadin protein (Sigma-Aldrich; 160 µg/ml), H_2O_2 (MP

Biomedicals; 100 µM), curcumin (Sigma-Aldrich; 10 µM) and pre-treated with 10 µM curcumin for 3 h followed by 160 µg/ml gliadin treatment for 24 h time period.

Preparation of whole-cell lysates, cytoplasmic extracts and nuclear extracts

The whole-cell lysates were prepared using the RIPA buffer [20 mM Tris-HCl (pH 7.4), 150 mM NaCl, 1 mM EDTA, 1% TritonX 100, and 10% SDS] supplemented with the protease inhibitor cocktail (Thermo Scientific) (Cholia et al. 2018). Nuclear extract was prepared by resuspending the cell pellet in a low salt buffer [20 mM HEPES (pH 7.9), 10 mM KCl, 1 mM EDTA, 1 mM PMSF, 10% glycerol and protease inhibitor cocktail] and incubated on ice for 10 min followed by centrifugation at 3000 rpm for 5 min at 4°C. The supernatant (cytosolic fraction having mitochondria) was collected in fresh tubes and stored at -20°C until further use. The pellet was washed twice with the low salt buffer and resuspended in high salt buffer [20 mM HEPES (pH 7.9), 10 mM KCl, 1 mM EDTA, 250 mM NaCl, 0.1% NP-40, 1 mM PMSF, 10% glycerol and protease inhibitor cocktail] and incubated on ice for 30 min with intermediate vortexing by the centrifugation at 12000 rpm for 10 min at 4°C, the supernatant (nuclear extract) was collected in fresh tubes and small aliquots were stored at -20°C for further experiments (Levrand et al. 2005).

Detection of Reactive Oxygen Species and Reactive Nitrogen Species

(a). H_2DCFDA assay: H_2DCFDA is a cell-permeable molecular probe used for the detection of reactive oxygen species (ROS) in cells. HCT-116 and HT-29 cells were cultured in 96 well plates at a density of 1×10^4 cells per well and overnight cultured cells were treated with different treatment for 24 h. After completion of treatment, cells were incubated with 1 µM of H_2DCFDA (Molecular Probes™ Invitrogen) for 1 h at 37°C in the dark. The unbound dye was removed, and cells were washed with PBS. The fluorescence intensity was recorded at an excitation/emission 485/535 nm using a microplate reader (BioTek® Synergy H1). Percent change in the level of ROS was calculated considering control as absolute. **(b). Nitroblue tetrazolium (NBT) based assay**: As a second measure for ROS NBT assay was accomplished as HCT-116, and HT-29 cells were cultured in 96 well plates at a cell density 1×10^4 cells per well, and overnight cultured cells were treated for 24 h. After completion of treatment, cells were incubated with freshly prepared NBT solution (0.1% w/v) for 3 h at 37°C (Sim Choi et al. 2006). The cells were washed twice with PBS and once with chilled methanol, the NBT deposited inside the cells were then dissolved in 2 M KOH and DMSO. The absorbance was read at 570 nm using a microplate reader (BioTek® Synergy H1) (Sarkar et al. 2017). **(c). DAF-FM assay**: The intercellular RNS level in the HCT-116 and HT-29 cells treated with gliadin, curcumin and their combinations and untreated as control cells were measured using cell-permeable fluorescent probe-based DAF-FM dye. Briefly, both HCT-116 and HT-29 cells were cultured in 96 well plates at a cell density 1×10^4 per well, and after the treatments, these cells were incubated with 20 µM DAF-FM (Molecular Probes™ Invitrogen) in the dark at 37°C for 1 h, the unbound dye was removed, and cells were washed with PBS. Fresh PBS was added, and fluorescence intensity was recorded at an excitation/emission wavelength at 478/515 nm using a microplate reader (BioTek® Synergy H1) again the plate was incubated in the dark at 37°C for 30 min, and another fluorescence intensity was recorded and the data represented as percentage change concerning control

(Dhiman, Garg 2014; Gupta et al. 2018). **(d). Nitric Oxide (NO) Level**: The secretory/extracellular nitric oxide (NO) levels were measured in the culture supernatants using Griess assay. Briefly, equal volumes of culture supernatant and Griess reagent (1% sulfanilamide and 0.1% of NEDD) were mixed. The absorbance of formed chromophore was recorded at 543 nm in a microplate reader (BioTek® Synergy H1). The nitrite content of each sample was evaluated from a standard curve obtained after linear regression made with the known concentration of sodium nitrate (0-100μM) and represented as the percent change in NO levels considering control as absolute (Gupta et al. 2018; Dhiman et al. 2013).

Assays to Examine the Mitochondrial Health

(a) Estimation of Mitochondrial ROS: HCT-116 and HT-29 cells were cultured on coverslips and treated for 24 h. After the treatment, cells were washed thrice with PBS and incubated with 5 μM MitoSOX red (Molecular Probes™ Invitrogen) for 30 min, which specifically detects mitochondrial ROS; ex/em: 510 nm/580 nm and 200 nM MitoTracker™ Red CMXRos (Molecular Probes™ Invitrogen) which specifically detect mitochondria; ex/em: 579nm/$_{599}$nm. Cells were washed thrice with PBS, and images were captured on Olympus SV-1200 Laser Scanning Confocal Microscope (Gupta et al. 2009). **(b) Determination of Mitochondrial Trans-membrane Potential (MTP)**: Mitochondrial Trans-membrane Potential (MTP) in both the cells lines HCT-116 and HT-29 after treatment was determined by using JC-1 dye (5,5’,6,6’-tetrachloro-1,1’,3,3’-tetraethylbenzimidazolylcarbocyanine iodide) (Molecular Probes™ Invitrogen). The cells were washed with PBS and incubated with 10 μM JC-1 dye for 30 min at 37°C in the dark. Cells were then washed thrice with PBS and resuspended in 100 μl of PBS. The JC-1 monomers (green) and JC-1 aggregates (red) were detected by FL1 and FL2 channels, respectively using BD Accuri C6 flow cytometer. MTP is calculated as a change in the green/red fluorescence intensity ratio (Gupta et al. 2009).

Antioxidant Enzymes Status

(a) SOD activity: Superoxide dismutase (SOD) activity was measured using pyrogallol auto-oxidation. Briefly, the reaction was started in a mixture having 0.1 mM sodium phosphate buffer (pH 8), 3 mM EDTA, and 8.1 mM pyrogallol with cell lysate. The change in absorbance was recorded at 0 min and 3 min at 420 nm wavelength using Shimadzu double-beam spectrophotometer against buffer as blank. SOD activity is expressed as Unit/mg of protein where one unit of SOD activity is defined as the amount of enzyme that causes half-maximal inhibition of auto-oxidation of pyrogallol. The final graph was plotted by converting it in percentage concerning untreated control cells (Gill et al. 2017). **(b) Catalase activity**: The activity of catalase enzyme was measured using the method as described by Aebi (1984) with slight modifications. Briefly, the reaction was started by adding the cell lysate into the reaction mixture having 10 mM H_2O_2 (substrate for Catalase) and 25 mM potassium phosphate buffer (pH 7.0). The activity was recorded for the degradation of H_2O_2 at 240 nm over 1 min using spectrophotometer (Aebi 1984). The activity of the enzyme was expressed as μM/min/mg protein using 39.4 $mM^{-1}cm^{-1}$ molar extinction coefficient (de Sousa et al. 2013). **(c) Total glutathione content**: Amount of total glutathione in the treated and untreated cells were measured using DTNB [(5,5'-Dithiobis-(2-nitrobenzoic acid)] also known as Ellman’s reagent. DTNB reacts with the glutathione and forms a yellow coloured 5-thionitrobenzoic acid

(TNB) product (Rahman et al. 2006). Briefly, 100 µg of total cell lysates were precipitated using 25% trichloroacetic acid (TCA), after centrifugation supernatant was mixed with 0.6 mM DTMB and incubated in the dark for 15 min at room temperature. Absorbance was recorded at 412 nm using a microplate reader (BioTek® Synergy H1). The total content of glutathione was estimated using linear regression mode with the known concentration of glutathione (0–50 µM) (Gill et al. 2017).

Determination of Oxidative Stress

(a) Protein oxidation: Oxidative stress induces carbonyl (CO) groups on side chains of proteins, which are chemically stable, it can be derivatized with 2,4-Dinitrophenylhydrazine (DNPH) into a detectable hydrazone product (Dalle-Donne et al. 2003). The protein lysates were mixed with DNPH solution (10 mM prepared in 2 N HCl) and incubated in the dark for 90 min with intermittent vortexing. The derivatized samples were precipitated with 20% TCA, followed by 2–3 time washing with ethanol/ethyl acetate (1:1, v/v). The pellet was dissolved in 6 M guanidium hydrochloride and absorbance were recorded at 385 nm using a microplate reader (BioTek® Synergy H1). The carbonyl content was calculated by applying the molar extinction coefficient of 22,000 $M^{-1}cm^{-1}$ (Gill et al. 2017). **(b) Lipid peroxidation**: Thiobarbituric acid reactive substances (TBARS) assay is one of the most widely used assays for measuring lipid peroxidation. During the persistent oxidative stress, polyunsaturated fatty acids get converted into malondialdehyde (MDA) via lipid peroxidation which is highly reactive and in the presence of thiobarbutaric acid (TBA) it forms pink coloured product (Siddique et al. 2012). Briefly, cell lysates (100 µg) were mixed with 15% TCA, 0.375% TBA and 0.25 M hydrochloric acid (HCl) followed by heating at 95°C for 45 min and cooling on ice for 30 min. The samples were then centrifuged at 1000 rpm for 10 min at 4°C, the absorption was recorded at 532 nm using microplate reader (BioTek® Synergy H1), and the TBARS content was calculated by using $1.56X10^5$ $M^{-1}cm^{-1}$ molar extinction coefficient, and results were expressed as nM/mg of protein (Gill et al. 2017). **(c) DNA damage detection**: The most common marker for oxidative stress-induced DNA damage is 8-oxo deoxyguanosine (8-oxo-dG) which is formed by the oxidation of guanine base. The oxidized DNA damage was detected with 8-oxo-dG antibody (Trevigen®), the cells were cultured on coverslips and treated with gliadin protein, curcumin and its combination. The cells were then fixed with chilled methanol and acetone (1:1 ratio) for 15 min and air-dried. The RNA was digested with RNase enzyme followed by *in-situ* DNA denaturation (0.15 N NaOH in 70% ethanol for 5 min). The cells were washed with 70% ethanol containing 4% formaldehyde (v/v), 50 % ethanol, 35 % ethanol and finally PBS for 2 min each and treated with protease K (TE buffer, pH 7.5) to digest the remaining proteins. The coverslips were blocked with 5% FBS for 1 h at 37°C, then incubated with primary antibody of 8-oxo-dG (Trivegen®, 1:250 dilution) in a humidified chamber. Cells were then incubated with Alexa Fluor 488 tagged secondary antibody (Invitrogen, 1/500 dilution) and nucleus was counterstained with Hoechst 33342 (Invitrogen). The images were captured using the OLYMPUS FV1200 Confocal Laser Scanning Microscope (Upadhyay et al. 2020).

Apurinic/Apyrimidinic Endonuclease (APE) activity assay

A 5' FAM labelled, 52 mer oligonucleotide having tetrahydrofuran (THF; analogue of AP site) at 31st nt (5′-GATCTGATTCCCCATCTCCTCAGTTTCACTTHFAGTGAAGGCATGCACCCTTCT-3′) and its complementary strand with 'A' opposite THF was procured from Imperial Life Sciences (ILS), India. These oligonucleotides are annealed in annealing buffer (10 mM Tris base, 50 mM NaCl, 0.1 mM EDTA). 4 pM duplex probe was incubated with freshly prepared nuclear lysates in a reaction buffer [50 mM Tris base (pH 8.5), 8 mM $MgCl_2$, 1 mM DTT, 1 mg/ml BSA, 4% Glycerol] at 37°C for 3 min. The reaction was stopped by adding 10 µl of stop buffer [10 mM EDTA, 3–4% Formaldehyde, 0.01% BPB, 30% Glycerol] followed by heating at 95°C for 5 min and kept it on ice till resolution of denaturing gel. The substrate and cleaved product was resolve on 12% polyacrylamide gel having 7 M urea in 1X TAE buffer. The fluorescence image was captured using the Bio-Rad Chemi Doc™ MP system, and densitometric analysis was done using Image Lab™ software of Bio-Rad version 5.2 (Mantha et al. 2008).

DNA-Protein interaction study: Electrophoretic Mobility Shift Assay (EMSA)

8 pM of duplex DNA probe (5' FAM labelled) containing the ARE sequence (5'-GATCTTTTATGCTGTGTCATGGTTT-3') was incubated with freshly prepared nuclear extracts (15 µg) in EMSA buffer (50 mM Tris pH 7.5, 10 mM $MgCl_2$, 0.1 mM KCl, 5 mM EDTA and 0.2 mM DTT) having 1 µg of acetylated BSA and 0.1 µl of poly (dI-dC) at 37°C for 15 min followed by electrophoresis on 6% native polyacrylamide gel in 1X TAE buffer. The fluorescence image was captured using the Bio-Rad Chemi Doc™ MP system, and densitometric analysis was done using Image Lab™ software of Bio-Rad version 5.2 (Mantha et al. 2008; Li et al. 2009).

Isolation of total RNA and Semi-quantitative RT-PCR analysis

Total RNA from the treated and untreated cells of HCT-116 and HT-29 was isolated using TRIzol® reagent (Invitrogen, USA) as per manufacturer's protocol. The quality of isolated RNA was quantified on NanoDrop 2000 (Thermo Scientific) and on denaturing agarose gel. Genomic DNA contamination was removed by using the TURBO DNA-free™ Kit (Invitrogen, USA), followed by synthesis of cDNA using iScript™ cDNA Synthesis Kit (Bio-Rad). The cDNA was used as a template for the amplification of the various genes by using gene-specific primer pairs (SOD-1, SOD-2, Catalase, GPx, NOS-2, NOS-3, Nrf-2, APE1) along with housekeeping genes (β-actin and GAPDH) as an endogenous control (**Table 1**). The PCR product was separated on 1.5% agarose gel contains ethidium bromide (EtBr) along with 100bp DNA ladder (TrackIt™100 bp DNA ladder, Invitrogen). The gel images were captured using the Bio-Rad Gel Doc™XR system, and densitometric analysis was done using Image Lab™ software of Bio-Rad version 5.2 (Gupta et al. 2018).

Table.1: List of primers used in present study.

S. No.	Gene Name	Forward Primer Sequence (5′-3′)	Reverse Primer Sequence (5′-3′)
1	SOD-1	GAAGGTGTGGGGAAGCATTA	ACATTGCCCAAGTCTCCAAC
2	SOD-2	CGTCACCGAGGAGAAGTACC	CTGATTTGGACAAGCAGCAA
3	Catalase	CGTGCTGAATGAGGAACAGA	AGTCAGGGTGGACCTCAGTG
4	GPx	CCAAGCTCATCACCTGGTCT	TCGATGTCAATGGTCTGGAA
5	NOS-2	CCAACAATGGCAACATCAGG	CGATGCACAGCTGAGTGAAT
6	NOS-3	GGCATCACCAGGAAGAAGA	CATGAGCGAGGCGGAGAT
7	Nrf-2	GAGAGCCCAGTCTTCATTGC	TGCTCAATGTCCTGTTGCAT
8	APE-1	TGGAATGTGGATGGGCTTCGAGCC	AAGGAGCTGACCAGTATTGATGA
9	β-actin	CTAAGTCATAGTCCGCCTAGAAGCA	TGGCACCCAGCACAATGAA
10	GAPDH	GCACCGTCAAGGCTGAGAAC	ATGGTGGTGAAGACGCCAGT

Western Blot Analysis

The whole-cell lysates were resolve on 10% denaturing SDS-PAGE and blotted onto a nitrocellulose membrane (Bio-Rad). Ponceau S staining was performed to confirm equal protein loading and transfer. The membrane was blocked with 5% nonfat dry milk (NFDM) in PBS having 0.1% Tween-20 (PSBT) for 2 h. Membranes were then incubated with primary antibody for anti-Nrf-2 (Santa Cruz Biotechnology, 1:1000 dilution), anti-APE1 (Biogenuix, 1:1000 dilution), anti-LaminB1 (Invitrogen, 1:750 dilution) and anti-β-actin (Invitrogen, 1:5000 dilution) in 5% NFDM-PSBT for overnight at 4°C. After three washes with PBST membrane was further incubated with respective horseradish peroxidase (HRP) conjugated anti-mouse/rabbit IgG secondary antibody (GeNei™, 1:5000) in 5% NFDM-PSBT. Peroxidase activity was captured using enhanced chemiluminescence reagent of Bio-Rad, and images were visualized using Bio-Rad Chemi Doc™ MP system and densitometric analysis was done using Image Lab™ software of Bio-Rad version 5.2.

Immunofluorescence Based Subcellular Distribution and Co-localization Studies of APE1 and Nrf-2

Subcellular distribution and co-localization of APE1, as well as Nrf-2, were examined using immunofluorescence based confocal laser scanning microscopy (CLSM). The HCT-116 and HT-29 cells were grown on sterile coverslips and treated as described in the previous section. After treatment, the cells were fixed with 4% paraformaldehyde (PFA) in PBS for 10 min at room temperature followed by three times wash with PBS. Cells were permeabilized with 0.1% Triton X-100 for 5 min at room temperature. After washing with PBS, cells were blocked with 10% FBS for 1 h at 37°C followed by overnight incubation with primary antibodies against anti-APE1 (Biogenuix, 1:100 dilution) and anti-Nrf-2 (Santa Cruz Biotechnology, 1:100) in a humidified chamber at 4°C. The glass coverslips were washed with PBS

three times and incubated at room temperature for 1 h with respective secondary antibodies, Alexa Fluor 488-conjugated anti-mouse IgG or Alexa Fluor 647-conjugated anti-rabbit IgG (Invitrogen, 1:100 dilution). After washing thrice, the coverslips were incubated in 0.1% solution of Hoechst 33342 (Invitrogen) at 37°C for 10–15 min. The glass coverslips were washed with PBS and mounted with a mounting solution (Sarkar et al. 2017). The fluorescence images were captured using a Laser Scanning Confocal Microscope (Olympus FV1200).

Co-Immunoprecipitation for confirming the interaction between APE1 and Nrf-2

In vitro interaction of APE1 and Nrf-2 was stabilized by a co-immunoprecipitation reaction of APE1 and Nrf-2 using magnetic beads coated with protein A/G from Bio-Rad (SureBeads™). Briefly, 100 µl of SureBeads™ were taken in 1.5 ml tube after thorough resuspension, magnetized beads and discard the supernatant and wash with PBST thrice. The beads were incubated with anti-APE1 antibody (10 µg) for 2 h at 4°C on rotation. After incubation beads were again magnetized and the supernatant was discarded followed by 3 times washing with PBST and again incubation with whole-cell lysates (about 300 µg) and rotate for overnight at 4°C. Beads were magnetized and discard the supernatant and wash thrice with PBST. Now, elute it in fresh Laemmli buffer having β-mercaptoethanol by heating at 70°C for 10 min followed by magnetization and collection of supernatant in a fresh tube. Again heat it at 95°C for 5 min and performed Western blotting as described above (in western blotting section) against primary antibody anti-Nrf-2 (Santa Cruz Biotechnology at 1:1000 dilution). After taking image again, the blot was stripped and reprobed with anti-β-actin antibody [Invitrogen at 1:5000 dilution] (Mantha et al. 2012; Thakur *et al.* 2020).

In-silico studies for understanding the interactions between APE1 and Nrf-2

The possible interacting partners of APE1 protein was predicted *in-silico* by using the STRING database (version 11.0). The database shows the direct and indirect association of proteins in over 2000 organisms. This database critically assesses the known interactions (from experimentally proven, curated database), and predict/possible interactions (from text mining, protein homology study, gene neighboring, co-occurrence and co-expression analysis (Sarkar et al. 2017).

Statistical Analysis

Experiments were performed in triplicates unless it specified, and data is represented as the mean value ± standard deviation (S.D), and statistical analysis of obtained data was done using student's t-test. The values of $p \leq 0.05$ were considered statistically significant.

Results

Measurement of Reactive Oxygen Species (ROS)

Fluorescence probe-based H_2DCFDA assay show increase in ROS level in gliadin and H_2O_2 treated HCT-116 and HT-29 cells. Whereas the cells when pre-treated (3 h) with curcumin followed by treatment with gliadin show decrease in ROS levels when compared with only gliadin treated cells in both the cell lines **(Figure: 1.A. i & ii).** NBT assay results show that in HCT-116 cells and HT-29 cells, ROS level increase significantly in gliadin and H_2O_2 treated cells whereas when the cells were pre-treated with curcumin followed by gliadin show decrease in ROS levels when compared with only gliadin treated cells in both the cell lines **(Sup. Figure: 1).**

Measurement of Reactive Nitrogen Species (RNS) and expression of Nitric Oxide Synthase (NOS) genes

The intracellular RNS level was measured using fluorescence probe based DAF-FM assay, and extracellular NO was estimated using Griess assay and semi-quantitative RT-PCR based NOS genes expression were also analyzed in the HCT-116 and HT-29 cell lines after 24 h treatment of gliadin, curcumin and their combinations. In both the cell lines (HCT-116 and HT-29) no change in intracellular RNS level was observed in gliadin, and H_2O_2 treated cells when compared with untreated control by using DAF-FM assay **(Figure: 1.B. i & ii)**. The extracellular NO level detected by Griess assay shows a slight increase in gliadin treated HCT-116 cells when compared with untreated control cells. The cells when pre-treated (3 h) with curcumin followed by treatment with gliadin protein a significant decrease in NO level was observed when compared with only gliadin treated cells **(Figure: 1.C.i)**; whereas no change was observed in HT-29 cells **(Figure: 1.C.ii)**.

The mRNA expression of *NOS-2/ inducible NOS* gene in the HCT-116 cells as well as in HT-29 cells is increased by 2 folds and 1.5 fold when cells are treated with gliadin protein and H_2O_2 respectively as compared with untreated control. The cells when pre-treated (3 h) with curcumin followed by treatment with gliadin showed a significant decrease as compared with only gliadin treated cells. Nearly the same trends were observed in HT-29 cells. The mRNA expression of *NOS-3/ endothelial NOS* gene in the HCT-116 and HT-29 cells is increased significantly when cells are treated with gliadin protein and H_2O_2, respectively. Whereas, when cells were pre-treated with curcumin followed by treatment with gliadin, a significant decrease in NOS-3 expression was observed when compared with only gliadin treated cells **(Figure: 1.D. i & ii)**.

Assessment of Mitochondrial ROS and Trans-membrane Potential

The ROS produced within the mitochondria upon treatment with gliadin in the HCT-116, and HT-29 cell lines were estimated via MitoSox™ dye (green), and mitochondria were tracked by MitoTracker™ dye (red) using fluorescence microscopy. Green fluorescence intensity is directly proportional to the ROS production within the mitochondria. The microphotographs obtained using confocal fluorescence microscope showed that the fluorescence intensity of green dye is high in gliadin treated HCT-116 and HT-29 cells, curcumin, and H_2O_2 treated cells also show an increase in green fluorescence intensity when compared with untreated control cells. In the cells pre-treated with curcumin followed by treatment with gliadin show relatively low green fluorescence signal as compared to only gliadin treated cells **(Figure:**

1.E. i & ii). Mitochondrial Transmembrane Potential (MTP) (ΔΨm), is a thoughtful parameter to sense the mitochondrial health which can be estimated using JC-1 dye which forms orange-red aggregates in healthy cells and remain green coloured monomers in unhealthy cells. The ratio of red to green fluorescence indicates mitochondrial health. The results show that red to green ratio decreases by 70–80% in HCT-116 and HT-29 cells when treated with gliadin protein and H_2O_2 as compared with untreated control cells; whereas the cells pre-treatment with curcumin followed by treatment with gliadin show about 2–4 fold increase in red to green fluorescence ratio as compared to only gliadin treated cells **(Figure: 1.E. iii & iv).**

Assessments of Cellular Antioxidant Enzyme Status

Superoxide dismutase Levels: The SOD enzyme activity was measured spectrophotometrically and was found to be increased by 37–40% in gliadin protein treated HCT-116 and HT-29 cells whereas, in H_2O_2 treated cells the SOD activity is increased by 34% when compared with untreated control cells. The cells, when pre-treated with curcumin followed by treatment with gliadin a significant decrease in SOD activity, was observed **(Figure: 2.A. i & ii)**. The mRNA expression of *SOD-1* gene was evaluated as a second measure both the cells. In HCT-116 cells, the expression is increased by 1.5 folds and 1.2 folds when cells are treated with gliadin protein and H_2O_2, respectively when compared with untreated control. The HCT-116 cells when pre-treated (3 h) with curcumin followed by treatment with gliadin protein show a decrease of 28% in SOD-1 expression was observed when compared with only gliadin treated cells. In HT-29 cells, the *SOD-1* gene expression was increased by about 3 folds and 2 folds when cells are treated with gliadin protein and H_2O_2, respectively as compared with untreated control cells. The HT-29 cells, when pre-treated (3 h) with curcumin followed by treatment with gliadin, show a decrease of 49% in SOD-1 expression when compared with only gliadin treated cells **(Figure: 2.D. i & ii)**.

Catalase Levels: The catalase enzyme activity in the HCT-116 cells was increased 3 folds in gliadin, and H_2O_2 treated cells when compared with untreated control cells. The HCT 116 cells, when pre-treated (3 h) with curcumin followed by treatment with gliadin a significant decrease of 38% in catalase activity was observed as compared with only gliadin treated HCT-116 cells **(Figure: 2.B.i)**. In HT-29 cells, catalase activity was increased by 2 folds in gliadin treated cells, and 77% in H_2O_2 treated cells as compared with untreated control cells. The cells pre-treated (3 h) with curcumin followed by treatment with gliadin a significant decrease of 25% in catalase activity was observed in HT-29 cells **(Figure: 2.B.ii)**. The mRNA expression of *catalase* gene in the HCT-116 and HT-29 cells showed augmented levels in cells treated with gliadin and H_2O_2 whereas no change is catalase expression was observed in both the cell lines when pre-treated with curcumin followed by gliadin treatment **(Figure: 2.D. i & ii)**.

Total glutathione content: The glutathione content which functions both as a free radical scavenger as well as a substrate for glutathione peroxidase, was measured in both the cell lines. In HCT-116 cells, 32% and 30% upsurge of glutathione was observed in cells treated with gliadin protein and H_2O_2 respectively when compared with untreated control HCT-116 cells. The cells when pre-treated (3 h) with curcumin followed by treatment with gliadin show a significant decrease of 23% in glutathione level when

compared with only gliadin treated cells **(Figure: 2.C. i)**. In HT-29 cells, glutathione was found to increase by 20% after gliadin treatment, and a 34% increase in H_2O_2 treated cells when compared with untreated control HT-29 cells. The cells pre-treated (3 h) with curcumin followed by treated with gliadin protein show a significant decrease of 22% in glutathione level HT-29 cells **(Figure: 2.C. ii)**. The mRNA expression of glutathione peroxidase gene in the HCT-116 cells, as well as HT 29 cells, increase by 2 folds when cells are treated with gliadin protein and H_2O_2. The cells when pre-treated (3 h) with curcumin followed by treatment with gliadin show a decrease of 42–59% when compared with only gliadin treated cells **(Figure: 2.D. i & ii)**.

Expression Analysis of Antioxidant Responsive Element (ARE) Regulatory Transcription Factor: Nrf-2

Nrf-2 is an important transcription factor which regulates the ARE genes and controls the associated pathways. Activation of this pathway protects cells from oxidative stress-induced diseases and maintains cellular homeostasis. The mRNA expression of *Nrf-2* gene in the HCT-116 cells augmented by 48% and 86% when cells are treated with gliadin and H_2O_2 respectively whereas in cells pre-treated (3 h) with curcumin followed by treatment with gliadin a decrease of 20% is observed when compared with only gliadin treated HCT-116 cells, a similar pattern in the of *Nrf-2* gene expression was observed in HT-29 cells **(Figure: 2.D. i & ii)**. The protein levels of Nrf-2 in the HCT-116 cells is increased by 2.5 folds, and 95% in gliadin and H_2O_2 treated cells respectively whereas pretreatment with curcumin reduces its levels by 38% when compared with only gliadin treated cells. In HT-29 cells, the expression of Nrf-2 was increased by 21% gliadin treated cells, whereas no change was observed in H_2O_2 treated cells as well as in HT-29 cells pre-treated with curcumin **(Figure: 2.E. i & ii)**.

Assessment of the oxidative stress as a consequence of gliadin toxicity

Protein oxidation was estimated by measuring carbonyl content which is formed due to the oxidative damage of protein molecules. The carbonyls content was estimated by DNPH based spectrophotometric method. In HCT-116 cells, 14% and 17% increase in protein carbonyls was observed in the gliadin, and H_2O_2 treated cells, respectively when compared with untreated control cells. The cells when pre-treated (3 h) with curcumin followed by treatment with gliadin protein showed a decrease of 14% in carbonyl content when compared with only gliadin treated cells. **(Figure: 3.A)**. In HT-29 cells 17% and 24% increase in protein carbonyls was observed when cells were treated with gliadin protein and H_2O_2 respectively and compared with untreated control cells whereas in the cells pre-treated (3 h) with curcumin followed by treatment with gliadin no change in protein carbonyls was observed when compared with only gliadin treated cells **(Figure: 3.B)**.

Lipid molecules of the cells (including cell membrane) get oxidized into malondialdehyde (MDA) during oxidative stress, which reacts with thiobarbituric acid (TBA) and forms thiobarbituric acid reactive species (TBARS). By quantifying the TBARS content, the cellular lipid peroxidation was estimated in both the cell lines. In the case of HCT-116 cells, 53% and 40% increase in lipid peroxidation content were observed in gliadin, and H_2O_2 treated cells, respectively when compared with untreated control cells. The cells, when

pre-treated with curcumin followed by treatment with gliadin a significant decrease of 29% in lipid peroxidation content, was observed when compared with only gliadin treated cells **(Figure: 3.C)**. In HT-29 cells 50% and 54% increase in lipid peroxidation was observed in cells were treated with gliadin and H_2O_2 respectively when compared with untreated control cells, whereas in curcumin pre-treated cells followed by treatment with gliadin 31% decrease in TBARS content when compared with only gliadin treated cells **(Figure: 3.D)**.

DNA damage due to oxidative stress leads to the formation of 8-oxo-dG by the oxidation of guanine residue which is detected by using a primary antibody against it and secondary antibody labelled with Alexa Fluor 488 (green fluorescence signal). The microphotographs from confocal fluorescence microscopy show that the intensity of green fluorescence is high in gliadin and H_2O_2 treated HCT-116 cells as compared to untreated control HCT-116 cells. In HCT-116 cells when pre-treated (3 h) with curcumin followed by treatment with gliadin protein show a significant decrease in green fluorescence intensity **(Figure: 3.E)**. In HT-29 cells the gliadin protein and H_2O_2 treated cells show high green fluorescence intensity as compared with untreated control HT-29 cells; whereas the HT-29 cells when pre-treated with curcumin followed by treatment with gliadin protein show a significant decrease in green fluorescence intensity **(Figure: 3.F)**.

Transcriptional and translational expression profiling of APE1: A key protein for the oxidized DNA damage repair via BER-pathway

ROS generated within the cells typically damage DNA by creating the abasic (apurinic/apyrimidinic) sites by oxidizing the bases. These oxidized bases get repaired via BER pathway which is facilitated by a multifunctional enzyme apurinic/apyrimidinic endonuclease 1 /redox effector factor-1 (APE1/Ref1). The change in the mRNA expression of *APE1* gene was evaluated by semi-quantitative RT-PCR method. The expression of *APE1* gene increases by 2 fold and 1.5 times in the gliadin protein and H_2O_2 treated cells, respectively. The pre-treatment with curcumin followed by treatment with gliadin show a significant decrease of 76% in the mRNA level of *APE1* in both HCT-116 and HT-29 cells **(Figure: 3.G & H)**. Western blotting was performed to detect the APE1 protein level. In HCT-116 cells as well as in HT 29 cells its expression was increased by 2 folds when the cells were treated with gliadin and H_2O_2 whereas cells when pre-treated with curcumin followed by treatment with gliadin decreased the APE1 level by 80% in HCT116 cells and 46% in HT 29 cells when compared with only gliadin treated cells **(Figure: 3.I & J)**.

AP Endonuclease activity

As a second measure to confirm the endonuclease activity of APE1 was performed. In HCT-116 cells, AP endonuclease activity increased by 65% to 3 folds in dose depended on manner after the treatment of 50, 100 and 150 μM H_2O_2, respectively. The AP endonuclease activity increased by 1.57 to 3 folds after the treatment of 80, 160, 240 μg/ml gliadin protein and slight increase was observed after the treatment of 5, 10, 15 μM of curcumin when compared with untreated controls. The cells when pre-treated (3 h) with different concentrations of curcumin (5, 10, 15 μM) followed by treatment of gliadin (160 μg/ml) 1.5

folds decrease in APE1 activity was observed in all the treatments (**Figure: 3.K & L).** In HT-29 cells, AP endonuclease activity is increased by 82% to 3 folds after the treatment of 50, 100 and 150 μM H_2O_2 respectively and is increased by 1.2–3 folds after the treatment of 80,160, 240 μg/ml gliadin protein. The activity is increased by 27%-83% after the treatment of 5, 10, 15 μM of curcumin whereas various curcumin concentrations (5, 10, 15 μM, 3 h) followed by treatment of gliadin (160 μg/ml) about 60%-100% decrease in AP endonuclease activity was observed when compared with only gliadin treated cells **(Figure: 3.M & N).**

Subcellular co-localization of APE1 and Nrf-2 proteins

APE1 and Nrf-2 are cytosolic proteins which translocate to the nucleus during oxidative stress condition. To observe the sub-cellular co-localization of these two proteins, immunofluorescence based confocal microscopy was performed. The microphotographs show that in both cells HCT 116 and HT 29 the expression of APE1 (red) and Nrf-2 (green) are high and yellow (a mixture of both red and green) colour appear when cells are treated with gliadin and H_2O_2. The co-localization (yellow colour) is less intense in cells pre-treated (3 h) with curcumin followed by treatment with gliadin protein when compared with only gliadin treated cells **(Figure: 4.A & B).** From the immunofluorescence based co-localization studies, it was found that during stress conditions, the expression of APE1 (red) and Nrf-2 (green) are high, and the protein gets translocated to the nucleus. For further confirmation, Western blot assay was performed with subcellular fractions (cytosolic and nuclear lysates) along with whole-cell lysates. The Western blot results show that both APE1 and Nrf-2 translocate from the cytoplasm to nucleus during gliadin stress but the cells when pre-treated with curcumin followed by treatment of gliadin the translocation is reduced **(Figure: 4.C & D).**

Interaction of Nrf-2 with ARE DNA fragment

EMSA is an *in vitro* technique used to study the physical interaction of DNA and protein. In this study, the interaction of ARE DNA fragment with Nrf-2 protein was studied which indicates that Nrf-2 (nuclear extracts) interact with the ARE DNA fragment and the interaction gets stronger with an increase during oxidative stress. In case of HCT-116 cells the interaction between Nrf-2 and ARE increased by 50% to 3 folds after the treatment of 50, 100 and 150 μM H_2O_2 and increases about 100% to 2.5 folds after the treatment of 80,160, 240 μg/ml gliadin; whereas the marginal increase was observed after the treatment of 5, 10, 15 μM of curcumin as compared with the untreated control cells. When cells were pre-treated with different concentrations of curcumin (5, 10, 15 μM, for 3 h) followed by treatment of gliadin (160 μg/ml) 87%, 64% and 36% decrease in the interaction was observed **(Figure: 4.E & F).** In HT-29 cells, the interaction of Nrf-2 with ARE elements increased by 68% to 2 folds after the treatment of 50, 100 and 150 μM H_2O_2, respectively, and increased by about 90% to 3 folds after the treatment of 80,160, 240 μg/ml gliadin; whereas no change was observed after the curcumin treatment alone (5, 10, 15 μM). When cells were pre-treated with different concentrations of curcumin (5, 10, 15 μM, for 3 h) followed by the treatment of gliadin (160 μg/ml) 100%, 74% and 12% decrease in the interaction were observed when compared only with the gliadin treated cells **(Figure: 4.G & H).**

Interaction study for APE1 and Nrf-2

The interaction between the APE1 and Nrf-2 protein was retrieved *in-silico* by using STRING database and found that the interaction of APE1 (APEX1) with Nrf-2 (NFE2L2) protein was mediated through some intermediate proteins like FEN1, RBX1, MCM2, KEAP1, CDKN1A and others **(Figure: 4.I).** For further confirmation of the physical interaction of APE1 and Nrf-2 protein co-immunoprecipitation (Co-IP) reaction was performed in both the cell lines which show that APE1 and Nrf-2 are potentially interacting partners and they physically interact with each other. This interaction gets stronger by gliadin stress, and again the pre-treatment of curcumin try to normalize this interaction in both the cell lines studied **(Figure: 4.J).**

Discussion

Gluten is the main seed storage protein of wheat, barley and rye, which are consumed worldwide. It has complex protein networks and composed of gliadin and glutenin parts (Wieser 2007). Out of these two, gliadin is the main causative factor for vigorous antigenic responses in the human intestine and play a key role in many wheat induced autoimmune diseases like celiac disease, non-celiac gluten sensitivity and other wheat associated allergies (Makharia et al. 2015; Barone et al. 2014; Gupta et al. 2018). Gliadin protein triggers the antigenic response mainly by producing excess ROS, RNS, disturbing cellular antioxidant defence system and chronic inflammation in the human intestine, which ultimately leads to the autoimmunity (Perez et al. 2017). In disease condition, the mucosa of the small intestine gets disrupted by autoantibodies and create avillus condition, which finally results in malabsorption, diarrhoea and hematochezia eventually resulting in colorectal cancer (Lasa et al. 2018; Pasha et al. 2016). Currently, the only effective treatment for these diseases is a strict lifelong gluten-free diet, i.e. excluding all wheat, rye and barley containing food products from the diet. The pathophysiology of wheat intolerance is not fully elucidated, and the beneficial role of phytochemical curcumin (herbal products) which is having a wide array of beneficial effects in human health are also not studied so for in these diseases.

The present study attempts to explore the *in vitro* molecular pathways of harmful effects of gliadin protein and also the role of curcumin (one of the most used spices) in maintaining the cellular homeostasis using human colon cancer cell lines (HCT-116 and HT-29) as an experimental model. (Gupta et al. 2018; Drago et al. 2006; Luciani et al. 2010) ROS/RNS are produced in the cells during normal metabolic pathways even they are the important secondary messengers and involve in many important cellular processes like vasodilation, killing the foreign pathogens, and others. Studies show that in hu1man gastrointestinal diseases, oxidative/nitrosative stress are the key factors for pathophysiology and disease severity (Moretti et al. 2018; Benedetti et al. 2018; Daulatzai 2015; Kaplan et al. 2017). Curcumin, a herbal supplement and principal constituent of turmeric (commonly used spice in Asian culinary), is a strong free radical scavenger and prevent ROS generation within the microenvironment of the cell (Amalraj et al. 2017; Sahu 2016). In the present study, it was found that ROS level was significantly reduced near to the level of untreated control HCT-116 and HT-29 cells when these cells were

pre-treated with the curcumin (10 μM) for 3 h followed by the exposure/treatment of gliadin. The pre-treatment of curcumin also significantly diminished the production of NO against gliadin exposure.

Gliadin protein is rich in proline and glutamine amino acids (a member of prolamin family) and the deficiency of prolyl endopeptidases enzyme; its digestion is not completed (Marti et al. 2005). Small under-digested gliadin proteins enter into the intestinal epithelial cells and lead to the activation of free radical activation pathways (Monguzzi et al. 2019) and resulting in an elevation in the level of free radical production in the intestinal cells. The free radicals result in the formation of ROS/RNS; their augmentation increases the level of many enzymatic and non-enzymatic antioxidant defence systems to protect the cells from detrimental effects of ROS. In the present study, the 1st line of antioxidant enzymes (SOD, Catalase and Glutathione) were estimated using biochemical and PCR based assays. The mRNA level and protein level of Nrf-2 (regulator of ARE) was also estimated. The results show that the levels of antioxidant enzymes are high in gliadin treated HCT-116 and HT-29 cells as compared with the untreated control cells whereas their levels are significantly decreased in the curcumin pre-treated cells as compared to only gliadin treated HCT-116 and HT-29 cells. These results are found to be in accordance of previous reports in which SOD levels reported to be increased tremendously in celiac patients (Patlevič et al. 2016; Stojiljković et al. 2009); and increased levels of reduced glutathione in active celiac patients (Stojiljković et al. 2012).

The persistent oxidative stress adversely affects the cellular macromolecules due to protein carbonylation, lipid peroxidation, oxidative and DNA damage. These consequences of oxidative stress were estimated and found that the level of protein carbonylation and lipid peroxidation (MDA content) significantly increased in gliadin challenged HCT-116 and HT-29 cells. These results are in accordance with the previous results, which show that the level of protein carbonylation and lipid peroxidation was significantly elevated in the blood of celiac patients (Moretti et al. 2018). The content of protein carbonylation and MDA was significantly reduced in the curcumin pre-treated HCT-116 and HT-29 cells as compared to only gliadin treated cells. These results suggest the role of phytochemical curcumin in lowering of gliadin induced oxidative stress responses in celiac patients.

Nucleic acid (DNA) play a critical role in normal cellular function and prone to interact with free radicals. These free radicals damage the DNA typically by creating the abasic apurinic/apyrimidinic DNA sites, oxidized purines, double-strand breaks and others. Out of this 8-oxo-dG (8-oxo- deoxyguanosine) are the major oxidative DNA base damage marker. In many previous studies, the presence of 8-oxo-dG was reported in the blood and urine samples of celiac patients (Szaflarska-Popławska et al. 2010; Ferretti et al. 2012). In the present study, the elevated level of 8-oxo-dG was found in both the cell lines HCT-116 and HT-29 after the treatment of gliadin which was significantly masked by the pre-treatment of curcumin.

Abasic sites, the DNA damage which is created by oxidative stress is mainly repaired via BER pathway by using APE1 enzyme along with other BER enzymes. APE1 is a multifunctional enzyme, along with its role in DNA base repair, cleaving of AP sites, it also helps in maintaining the cellular redox homeostasis by interacting and activating many key transcription factors like Nrf-2, AP-1, NF-κB, p53, HIF1α and others

(Sarkar et al. 2017; Thakur et al. 2018; Manguinhas et al. 2020). In the present study transcriptional and translational levels (expression profiling) of APE1, endonuclease activity and its redox function were performed in HCT-116 and HT-29 cells in the presence of gliadin, curcumin and their combinations. The level of APE1 was increased upon gliadin stress along with increased endonuclease activity. These results support preexisting knowledge of multifunctional nature of APE1 upon gliadin induced oxidative stress its expression increased which might be associated with helping in DNA repair mechanism, enhanced expression, activation and subcellular translocation of different key transcription factors like Nrf-2 (Perez et al. 2017).

Nuclear factor (erythroid-derived 2)-like 2 (Nrf-2) also known as NFE2L2, which regulates many aspects of cellular homeostasis mainly against the oxidative stress and inflammation (Taguchi et al. 2011). It activates the antioxidant response element (ARE), which is a promoter of phase-II antioxidant enzyme responsible for scavenging the excess of ROS/RNS, prevent the oxidative stress and protect against the cellular damage (Kansanen et al. 2013; Zhang et al. 2019). The transcriptional and translational expression level profiling of Nrf-2 examined in present work was increased in both the HCT-116 and HT-29 cell lines after treatment of gliadin protein whereas it was decreased in curcumin pre-treated HCT-116 and HT-29 cells as compared to only gliadin treated cells. Nrf-2 is present in the cytoplasm as an inactive complex attached with Kelch-like ECH-associated protein-1 (Keap-1), during oxidative stress; this complex gets dissociated and Nrf-2 translocates to the nucleus (Shan et al. 2015). In the nucleus, Nrf-2 gets attached with the Maf protein and activate ARE. Reports suggest that it also interacts with the multifactorial enzyme APE1 and helps in managing the oxidative stress (Sarkar et al. 2017) to further confirm it in gliadin induced toxicity confocal microscopy, Western blotting, EMSA and co-immunoprecipitation were performed. From the confocal microscopy data, it is apparent that upon gliadin induced oxidative stress the nuclear translocation of APE1 and Nrf-2 increases which is further confirmed by the Western blot of subcellular fractions using nuclear lysates, cytosolic fractions and whole-cell lysates. Nrf-2 is a transcription factor which directly regulates many other proteins associated with oxidative stress by binding with ARE (Lacher, Slattery 2016; Zhang et al. 2019). The EMSA results show that Nrf-2 protein directly interacts with the ARE-DNA sequence and its binding efficiency observed is directly proportional to the oxidative stress in both the HCT-116 and HT-29 cell lines.

From the literature and STRING database analysis, it was predicted that these two critical proteins are directly interacting with each other. Further, the physical interaction was confirmed in *vitro* conditions using co-immunoprecipitation (Co-IP) experiment. Previous reports have also identified an interaction between these two pathways in primary pancreatic ductal adenocarcinoma tumour cells and suggested to be playing a crucial role in overcoming the resistance against experimental drugs targeting Ref-1 activity. The present study and other studies from our group (Sarkar et al. 2017; Thakur *et al.* 2020) advocate the physical interaction between APE1 and Nrf-2 which is associated with regulation of many cell survival pathways leading to the re-establishment of cellular homeostasis against oxidative stress. However, the specific transcription factors and their downstream translational implications need to be elucidated further in the human pathophysiology diseases including wheat protein-induced allergies.

Summary And Conclusion

The experimental data presented suggests that pure gliadin protein induces oxidative stress by increasing ROS/RNS and disturbs the antioxidant system which damages the cellular macromolecules in both the human colon cancer HCT-116 and HT-29 cell lines. Additionally, the pivotal role of APE1 and Nrf-2 proteins along with their subcellular localization during the oxidative stress being demonstrated. This study also establishes the interaction of these two proteins and their key role in maintaining the cellular homeostasis against gliadin induced oxidative stress **(Figure: 5).** Further, the role of curcumin was investigated which significantly revitalizes the colon cancer cells against gliadin induced stress and modulated its adverse effects via DNA repair pathways and oxidative stress which is evident through the cross-talk between two crucial proteins of these pathways APE1 and Nrf-2 hence suggesting the role of curcumin based management of wheat intolerance diseases like celiac disease.

Declarations

Acknowledgement

KBG acknowledges the Indian Council of Medical Research (ICMR), New Delhi for providing financial assistance in the form of JRF/SRF. Central Instrumentation Laboratory (CIL), Central University of Punjab, Bathinda for providing instrumentation facility being thankfully acknowledged.

Funding: KBG has been supported by Indian Council of Medical Research (ICMR), New Delhi for the financial assistance in the form of JRF/SRF.

Conflicts of interest/Competing interests: Authors do not have any conflict of interest to declare.

Availability of data and material: The original data is with the corresponding author and can be provided as and when required.

Authors' contributions: Conceptualization, MD; methodology, investigation writing – original draft, KBG: editing, funding acquisition and supervision, MD &AKM

Ethics approval: Not required

Consent to participate: Not required

Consent for publication: **Not required**

Code availability: None

References

1. Aebi H (1984) Catalase in vitro. Methods in enzymology. Elsevier, pp 121–126

2. Amalraj A, Pius A, Gopi S, Gopi S (2017) Biological activities of curcuminoids, other biomolecules from turmeric and their derivatives–A review. Journal of Traditional Complementary Medicine 7(2):205–233
3. Barone MV, Troncone R, Auricchio S (2014) Gliadin peptides as triggers of the proliferative and stress/innate immune response of the celiac small intestinal mucosa. Int J Mol Sci 15(11):20518–20537
4. Benedetti E, Viscido A, Castelli V, Maggiani C, d'Angelo M, Di Giacomo E et al (2018) Mesalazine treatment in organotypic culture of celiac patients: Comparative study with gluten free diet. J Cell Physiol 233(6):4383–4390
5. Cholia RP, Dhiman M, Kumar R, Mantha AK (2018) Oxidative stress stimulates invasive potential in rat C6 and human U-87 MG glioblastoma cells via activation and cross-talk between PKM2, ENPP2 and APE1 enzymes. Metab Brain Dis 33(4):1307–1326
6. Dalle-Donne I, Rossi R, Giustarini D, Milzani A, Colombo R (2003) Protein carbonyl groups as biomarkers of oxidative stress. Clin Chim Acta 329(1–2):23–38
7. Daulatzai MA. Non-celiac gluten sensitivity triggers gut dysbiosis, neuroinflammation, gut-brain axis dysfunction, and vulnerability for dementia. CNS & Neurological Disorders-Drug Targets (Formerly Current Drug Targets-CNS & Neurological Disorders). 2015;14(1):110–31
8. de Sousa A, Teixeira J, Regueiras MT, Azenha M, Silva F, Fidalgo F (2013) Metalaxyl-induced changes in the antioxidant metabolism of Solanum nigrum L. suspension cells. Pestic Biochem Physiol 107(2):235–243
9. Dhiman M, Garg NJ (2014) P47phox−/− mice are compromised in expansion and activation of CD8 + T cells and susceptible to Trypanosoma cruzi infection. PLoS Pathog 10(12):e1004516
10. Dhiman M, Wan X, Popov VL, Vargas G, Garg NJ (2013) Mn SOD tg Mice Control Myocardial Inflammatory and Oxidative Stress and Remodeling Responses Elicited in Chronic Chagas Disease. Journal of the American Heart Association 2(5):e000302
11. Drago S, El Asmar R, Di Pierro M, Grazia Clemente M, Sapone ATA, Thakar M et al (2006) Gliadin, zonulin and gut permeability: Effects on celiac and non-celiac intestinal mucosa and intestinal cell lines. Scand J Gastroenterol 41(4):408–419
12. Ferretti G, Bacchetti T, Masciangelo S, Saturni L (2012) Celiac disease, inflammation and oxidative damage: a nutrigenetic approach. Nutrients 4(4):243–257
13. Gill I, Kaur S, Kaur N, Dhiman M, Mantha AK (2017) Phytochemical ginkgolide B attenuates amyloid-β 1–42 induced oxidative damage and altered cellular responses in human neuroblastoma SH-SY5Y cells. J Alzheimers Dis 60(s1):S25–S40
14. González-Reyes S, Guzmán-Beltrán S, Medina-Campos ON, Pedraza-Chaverri J. Curcumin pretreatment induces Nrf2 and an antioxidant response and prevents hemin-induced toxicity in primary cultures of cerebellar granule neurons of rats. Oxidative Medicine and Cellular Longevity. 2013;2013

15. Gupta KB, Upadhyay S, Saini RG, Mantha AK, Dhiman M (2018) Inflammatory response of gliadin protein isolated from various wheat varieties on human intestinal cell line. J Cereal Sci 81:91–98
16. Gupta S, Bhatia V, Wen J-j, Wu Y, Huang M-H, Garg NJ (2009) Trypanosoma cruzi infection disturbs mitochondrial membrane potential and ROS production rate in cardiomyocytes. Free Radic Biol Med 47(10):1414–1421
17. Kansanen E, Kuosmanen SM, Leinonen H, Levonen A-L (2013) The Keap1-Nrf2 pathway: mechanisms of activation and dysregulation in cancer. Redox Biology 1(1):45–49
18. Kaplan M, Ates I, Yüksel M, Ozin YO, Akpinar MY, Topcuoglu C et al (2017) The role of oxidative stress in the etiopathogenesis of gluten-sensitive enteropathy disease. Journal of Medical Biochemistry 36(3):243–250
19. Lacher SE, Slattery M (2016) Gene regulatory effects of disease-associated variation in the NRF2 network. Current Opinion in Toxicology 1:71–79
20. Lasa J, Rausch A, Bracho LF, Altamirano J, Speisky D, de Dávila MTG et al. Colorectal Adenoma Risk Is Increased among Recently Diagnosed Adult Celiac Disease Patients. Gastroenterology Research and Practice. 2018;2018
21. Levrand S, Pesse B, Feihl F, Waeber B, Pacher P, Rolli J et al (2005) Peroxynitrite is a potent inhibitor of NF-κB activation triggered by inflammatory stimuli in cardiac and endothelial cell lines. J Biol Chem 280(41):34878–34887
22. Li C-Q, Kim MY, Godoy LC, Thiantanawat A, Trudel LJ, Wogan GN. Nitric oxide activation of Keap1/Nrf2 signaling in human colon carcinoma cells. Proceedings of the National Academy of Sciences, USA. 2009;106(34):14547-51
23. Liu L, Ikeda TM, Branlard G, Peña RJ, Rogers WJ, Lerner SE et al (2010) Comparison of low molecular weight glutenin subunits identified by SDS-PAGE, 2-DE, MALDI-TOF-MS and PCR in common wheat. BMC Plant Biol 10(1):124
24. Luciani A, Villella VR, Vasaturo A, Giardino I, Pettoello-Mantovani M, Guido S et al (2010) Lysosomal accumulation of gliadin p31–43 peptide induces oxidative stress and tissue transglutaminase-mediated PPARγ downregulation in intestinal epithelial cells and coeliac mucosa. Gut 59(3):311–319
25. Makharia A, Catassi C, Makharia GK (2015) The overlap between irritable bowel syndrome and non-celiac gluten sensitivity: a clinical dilemma. Nutrients 7(12):10417–10426
26. Manguinhas R, Fernandes AS, Costa JG, Saraiva N, Camões SP, Gil N et al (2020) Impact of the APE1 Redox Function Inhibitor E3330 in Non-Small Cell Lung Cancer Cells Exposed to Cisplatin: Increased Cytotoxicity and Impairment of Cell Migration and Invasion. Antioxidants 9(6):550
27. Mantha AK, Dhiman M, Taglialatela G, Perez-Polo RJ, Mitra S (2012) Proteomic study of amyloid beta (25–35) peptide exposure to neuronal cells: Impact on APE1/Ref-1's protein–protein interaction. J Neurosci Res 90(6):1230–1239
28. Mantha AK, Oezguen N, Bhakat KK, Izumi T, Braun W, Mitra S (2008) Unusual role of a cysteine residue in substrate binding and activity of human AP-endonuclease 1. J Mol Biol 379(1):28–37

29. Marti T, Molberg Ø, Li Q, Gray GM, Khosla C, Sollid LM (2005) Prolyl endopeptidase-mediated destruction of T cell epitopes in whole gluten: chemical and immunological characterization. J Pharmacol Exp Ther 312(1):19–26
30. Molina-Infante J, Santolaria S, Sanders D, Fernández-Bañares F (2015) Systematic review: noncoeliac gluten sensitivity. Alimentary Pharmacology Therapeutics 41(9):807–820
31. Monguzzi E, Marabini L, Elli L, Vaira V, Ferrero S, Ferretti F et al (2019) Gliadin effect on the oxidative balance and DNA damage: An in-vitro, ex-vivo study. Digestive Liver Disease 51(1):47–54
32. Moretti S, Mrakic-Sposta S, Roncoroni L, Vezzoli A, Dellanoce C, Monguzzi E et al. Oxidative stress as a biomarker for monitoring treated celiac disease. Clinical and Translational Gastroenterology. 2018;9(6)
33. Pasha I, Saeed F, Sultan MT, Batool R, Aziz M, Ahmed W (2016) Wheat allergy and intolerence; Recent updates and perspectives. Crit Rev Food Sci Nutr 56(1):13–24
34. Patlevič P, Vašková J, Švorc P Jr, Vaško L, Švorc P (2016) Reactive oxygen species and antioxidant defense in human gastrointestinal diseases. Integrative Medicine Research 5(4):250–258
35. Perez S, Talens-Visconti R, Rius-Perez S, Finamor I, Sastre J (2017) Redox signaling in the gastrointestinal tract. Free Radic Biol Med 104:75–103
36. Pinkus R, Weiner LM, Daniel V (1996) Role of oxidants and antioxidants in the induction of AP-1, NF-κB, and glutathione S-transferase gene expression. J Biol Chem 271(23):13422–13429
37. Rahman I, Kode A, Biswas SK (2006) Assay for quantitative determination of glutathione and glutathione disulfide levels using enzymatic recycling method. Nat Protoc 1(6):3159
38. Sahu PK (2016) Design, structure activity relationship, cytotoxicity and evaluation of antioxidant activity of curcumin derivatives/analogues. Eur J Med Chem 121:510–516
39. Sarkar B, Dhiman M, Mittal S, Mantha AK (2017) Curcumin revitalizes Amyloid beta (25–35)-induced and organophosphate pesticides pestered neurotoxicity in SH-SY5Y and IMR-32 cells via activation of APE1 and Nrf2. Metab Brain Dis 32(6):2045–2061
40. Scherf KA (2019) Immunoreactive cereal proteins in wheat allergy, non-celiac gluten/wheat sensitivity (NCGS) and celiac disease. Current Opinion in Food Science 25:35–41
41. Shan J-L, He H-T, Li M-X, Zhu J-W, Cheng Y, Hu N et al (2015) APE1 promotes antioxidant capacity by regulating Nrf-2 function through a redox-dependent mechanism. Free Radic Biol Med 78:11–22
42. Siddique YH, Ara G, Afzal M (2012) Estimation of lipid peroxidation induced by hydrogen peroxide in cultured human lymphocytes. Dose-Response 10(1):1–10
43. Sim Choi H, Woo Kim J, Cha YN, Kim C (2006) A quantitative nitroblue tetrazolium assay for determining intracellular superoxide anion production in phagocytic cells. Journal of Immunoassay Immunochemistry 27(1):31–44
44. Singh P, Arora A, Strand TA, Leffler DA, Catassi C, Green PH et al (2018) Global prevalence of celiac disease: systematic review and meta-analysis. Clin Gastroenterol Hepatol 16(6):823–836. e2

45. Stojiljković V, Pejić SA, Kasapović J, Gavrilović L, Stojiljković S, Nikolić D et al (2012) Glutathione redox cycle in small intestinal mucosa and peripheral blood of pediatric celiac disease patients. Anais da Academia Brasileira de Ciencias 84(1):175–184
46. Stojiljković V, Todorović A, Pejić S, Kasapović J, Saičić ZS, Radlović N et al (2009) Antioxidant status and lipid peroxidation in small intestinal mucosa of children with celiac disease. Clin Biochem 42(13–14):1431–1437
47. Sun Z, Zhang S, Chan JY, Zhang DD (2007) Keap1 controls postinduction repression of the Nrf2-mediated antioxidant response by escorting nuclear export of Nrf2. Mol Cell Biol 27(18):6334–6349
48. Szaflarska-Popławska A, Siomek A, Czerwionka-Szaflarska M, Gackowski D, Różalski R, Guz J et al (2010) Oxidatively damaged DNA/oxidative stress in children with celiac disease. Cancer Epidemiology Prevention Biomarkers 19(8):1960–1965
49. Taguchi K, Motohashi H, Yamamoto M (2011) Molecular mechanisms of the Keap1–Nrf2 pathway in stress response and cancer evolution. Genes Cells 16(2):123–140
50. Thakur S, Dhiman M, Mantha AK (2018) APE1 modulates cellular responses to organophosphate pesticide-induced oxidative damage in non-small cell lung carcinoma A549 cells. Mol Cell Biochem 441(1–2):201–216
51. Thakur S, Dhiman M, Tell G, Mantha AK (2015) A review on protein–protein interaction network of APE1/Ref-1 and its associated biological functions. Cell Biochem Funct 33(3):101–112
52. Thakur S, Sarkar B, Dhiman M, Mantha AK. Organophosphate-pesticides induced survival mechanisms and APE1-mediated Nrf2 regulation in non-small-cell lung cancer cells. Journal of Biochemical and Molecular Toxicology.2020;e22640
53. Upadhyay S, Mantha AK, Dhiman M. Glycyrrhiza glabra (Licorice) root extract attenuates doxorubicin-induced cardiotoxicity via alleviating oxidative stress and stabilising the cardiac health in H9c2 cardiomyocytes. Journal of Ethnopharmacology. 2020;112690
54. Wieser H (2007) Chemistry of gluten proteins. Food Microbiol 24(2):115–119
55. Zhang H, Zheng W, Feng X, Yang F, Qin H, Wu S et al (2019) Nrf2–ARE signaling acts as master pathway for the cellular antioxidant activity of fisetin. Molecules 24(4):708

Figures

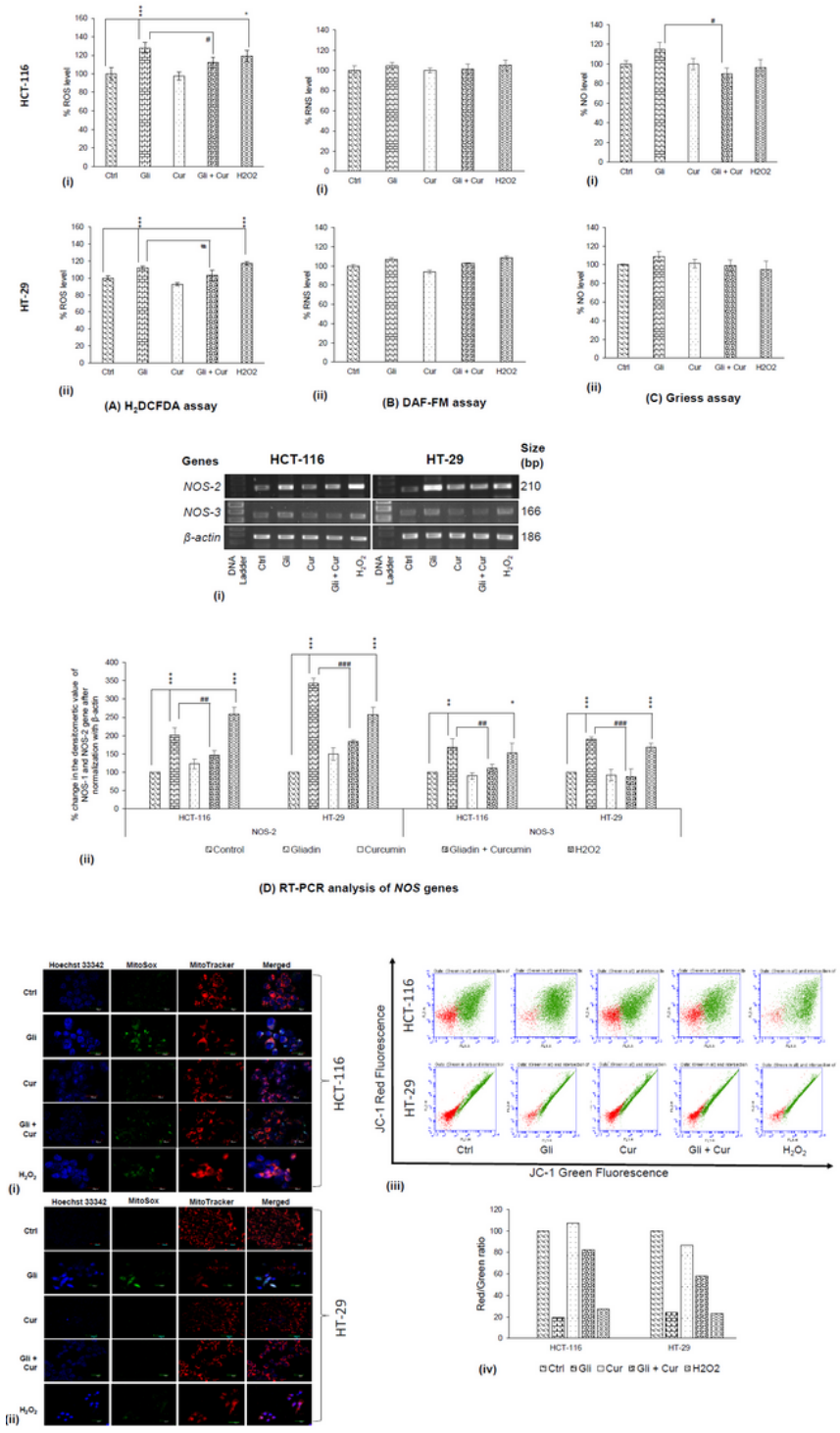

Figure 1

Estimation of Oxidative and Nitosative Stress. (A): Reactive Oxygen Species (ROS) production in both HCT-116 and HT-29 cells was estimated by using a molecular probe (H2DCFDA) based assay. The relative fluorescence unit (RFU) converted to percent ROS in: (i) HCT-116 cells, and (ii) HT-29 cells after the treatment of gliadin, curcumin and their combinations (3 h pretreatment of curcumin) and H2O2 for 24 h. (B): Intracellular reactive nitrogen species (RNS) was estimated using molecular probe DAF-FM. The

relative fluorescence unit (RFU) converted to percent RNS in: (i) HCT-116 cells and (ii) HT-29 cells. (C): Extracellular NO estimation through Griess assay in: (i) HCT-116 cells and (ii) HT-29 cells. (D): The mRNA expression profile of NOS-2 (i-NOS) and NOS-3 (e-NOS) was estimated through semi-quantitative RT-PCR using β-actin as an internal control, (i) representative agarose gel images and (ii) densitometric analysis after the normalization with the expression of β-actin. The results are expressed as the mean of percent change ± standard deviation (n=3). ***P≤0.005, *P≤0.05 (Control vs. Gliadin/Curcumin/H2O2 in both the cell lines), #P≤0.05 (Gliadin vs. Gliadin+Curcumin in both the cell lines). (E): Mitochondrial ROS was detected through MitoSoxTM probe and mitochondrial membrane potential was estimated through MitoTracker and JC-1 dye. Representative confocal microscopy image of Mitochondria stained with MitoTracker (red colour) and Mitochondrial ROS (Green colour) in: (i) HCT-116 cells, (ii) HT-29 cells after the treatment of gliadin, curcumin and their combinations (3 hr pretreatment of curcumin) and H2O2 for 24 h; (iii) Flow cytometry-based analysis of the mitochondrial transmembrane potential by using JC-1 dye in both HCT-116 and HT-29 cells, and (iv) Bar graph showing the ratio of Red/Green JC-1 dye after the treatment of gliadin, curcumin and their combinations (3 h pretreatment of curcumin) and H2O2 for 24 h.

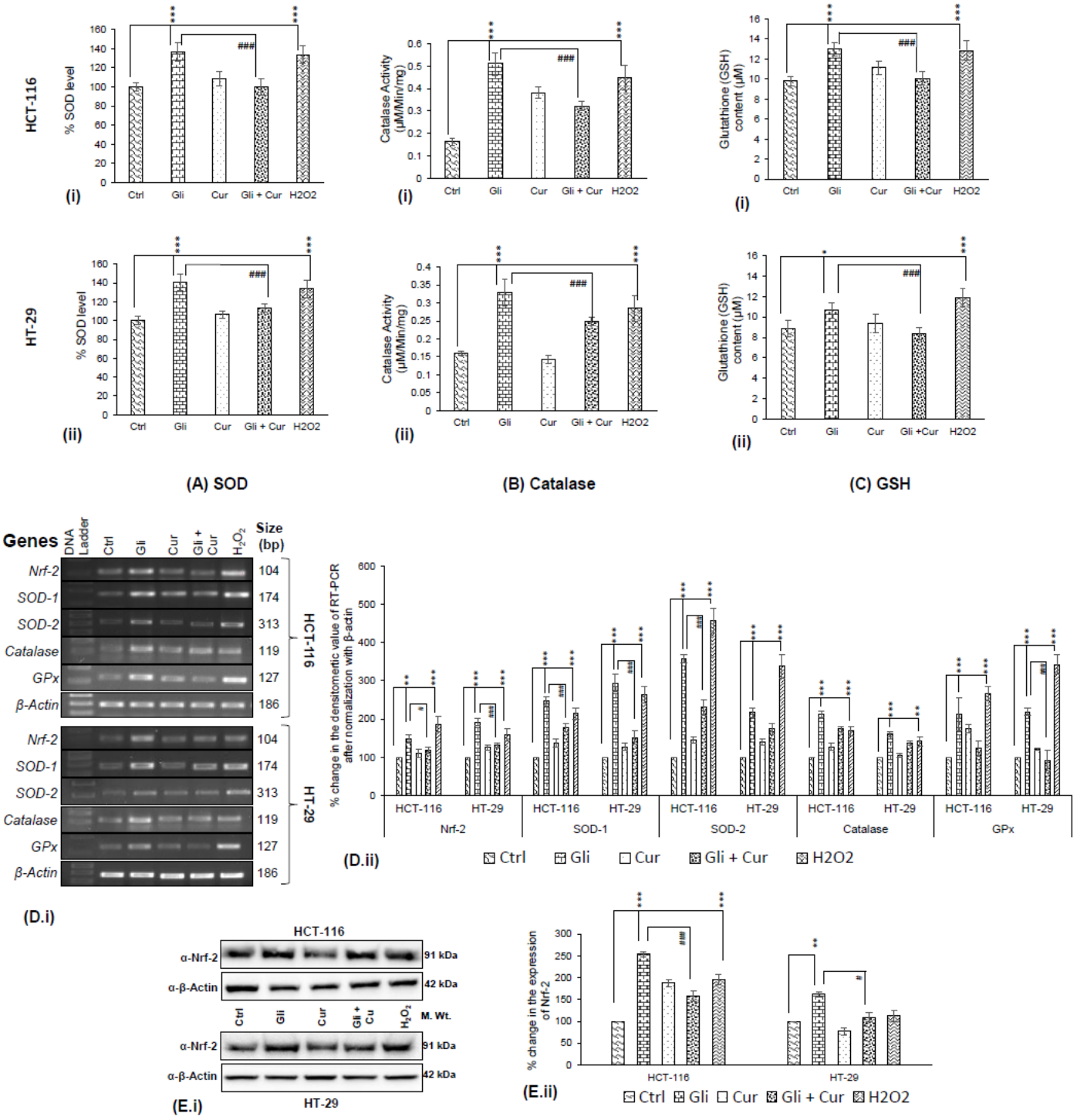

Figure 2

Cellular Antioxidant Status: The expression profile of antioxidant enzymes and their enzyme activity were determined after the treatment of gliadin, curcumin and their combinations (3 h pretreatment of curcumin) and H2O2 for 24 h. (A) Spectrophotometry based total SOD activity in whole cell lysates of: (i) HCT-116 cells, and (ii) HT-29 cells. (B) Spectrophotometry based Catalase activity in: (i) HCT-116 cells, and (ii) HT-29 cells. (C) Spectrophotometry based Glutathione (GSH) content in the whole cell lysates: (i)

in HCT-116 cells, and (ii) in HT-29 cells were examined. (D) The mRNA expression profile of different antioxidant genes viz. SOD-1, SOD-2, Catalase, GPx and Nrf-2 were evaluated through semi-quantitative RT-PCR method by keeping β-actin as an internal control; (i) representative agarose gel images, and (ii) densitometric analysis of gel images after the normalization with the expression of β-actin. (E) The protein expression profiling of Nrf-2 protein was carried out through Western blot using β-actin as an internal control in both the cell lines; (i) representative immunoblot images and (ii) densitometric analysis of these images after normalization with the expression of β-actin. Results were expressed as mean ± standard deviation (n=3). ***P≤0.005, *P≤0.05 (Control vs. Gliadin/Curcumin/H2O2 in both the cell lines), #P≤0.05 (Gliadin vs. Gliadin+Curcumin in both the cell lines).

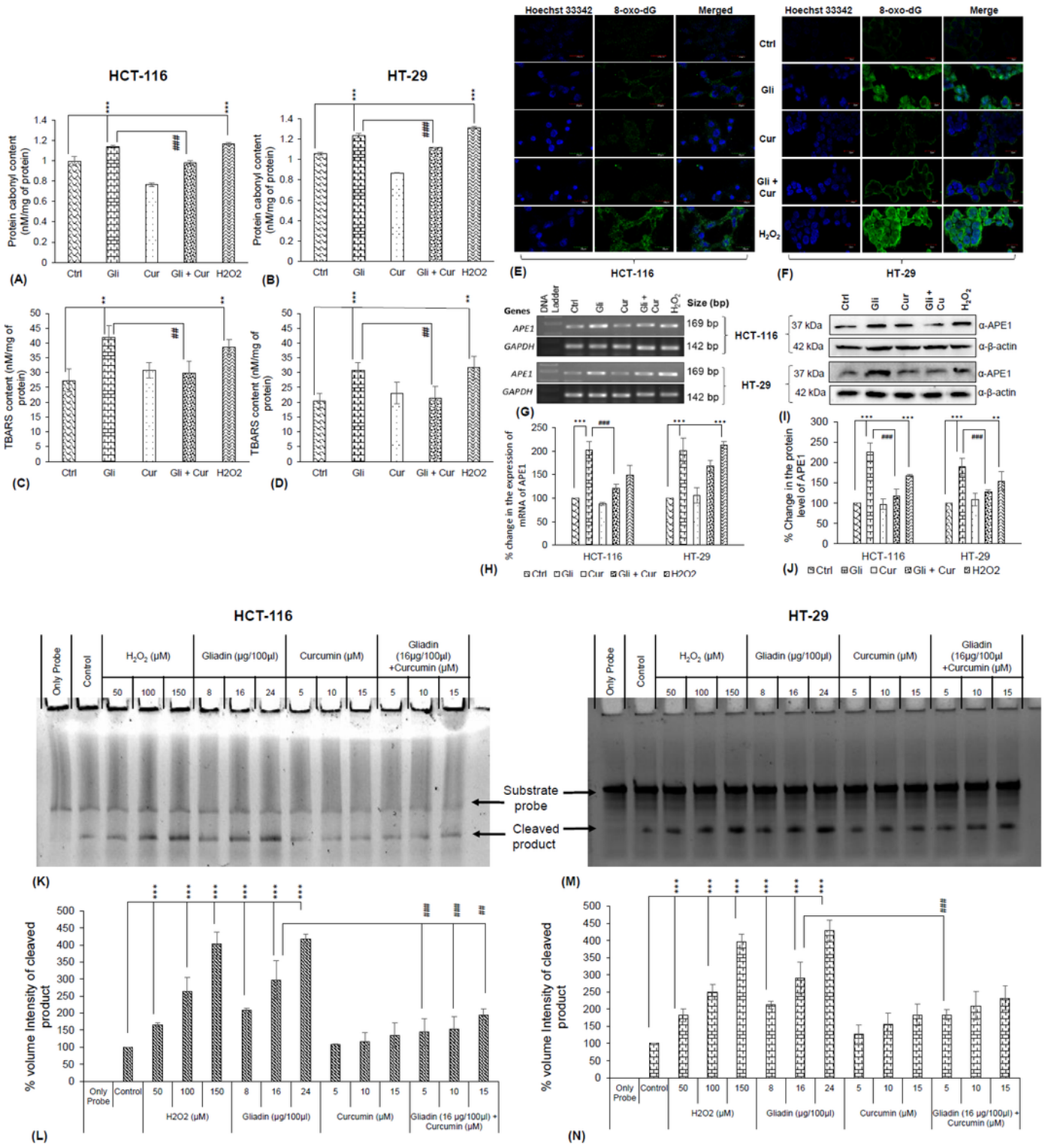

Figure 3

Detection of Oxidative Stress as Consequences of Gliadin induced Oxidative Stress: The adverse effects of these oxidative/nitrosative stress on different cellular macromolecules was estimated after the treatment of gliadin, curcumin and their combinations (3 h pretreatment of curcumin) and H2O2 for 24 h. Protein carbonylation (a marker for protein oxidation) content (nM/mg of protein) in: (A) HCT-116, and (B) HT-29 cells was measured spectrophotometrically. Thiobarbituric acid reactive substances (TBARS; a

marker of lipid oxidation) content (nM/mg of protein) in: (C) HCT-116, and (D) HT-29 cells was measured spectrophotometrically. Immunofluorescence based detection of oxidative stress-induced DNA base damage (8-oxo-dG site) was performed using confocal microscopy. The representative images are shown for: (E) HCT-116, and (F) HT-29 cells. The mRNA expression profile of APE1 gene (a key enzyme of DNA base damage repair) was performed by semi-quantitative RT-PCR using GAPDH as an internal control, (G) representative agarose gel image for APE1 gene expression, and (H) densitometric analysis of gel images after the normalization with the expression of GAPDH in both the cell lines. (I) The protein expression profile of APE1 protein was performed by Western blot using β-actin as an internal control, and (J) densitometric analysis of after normalization with the expression of β-actin in both the cell lines. The ability to abasic (AP) site repair of different nuclear extracts prepared after different treatments of both the cell lines was estimated using AP-endonuclease activity assay: (K) the representative gel images, and L) densitometric data of cleaved product for HCT-116 cells, and (M) The representative gel images, and (N) densitometric data of the cleaved product for HT-29 cells. The results were expressed as mean ± standard deviation (n=3). ***P≤0.005, *P≤0.05 (Control vs. Gliadin/Curcumin/H2O2 in both the cell lines), #P≤0.05 (Gliadin Vs. Gliadin+Curcumin in both the cell lines).

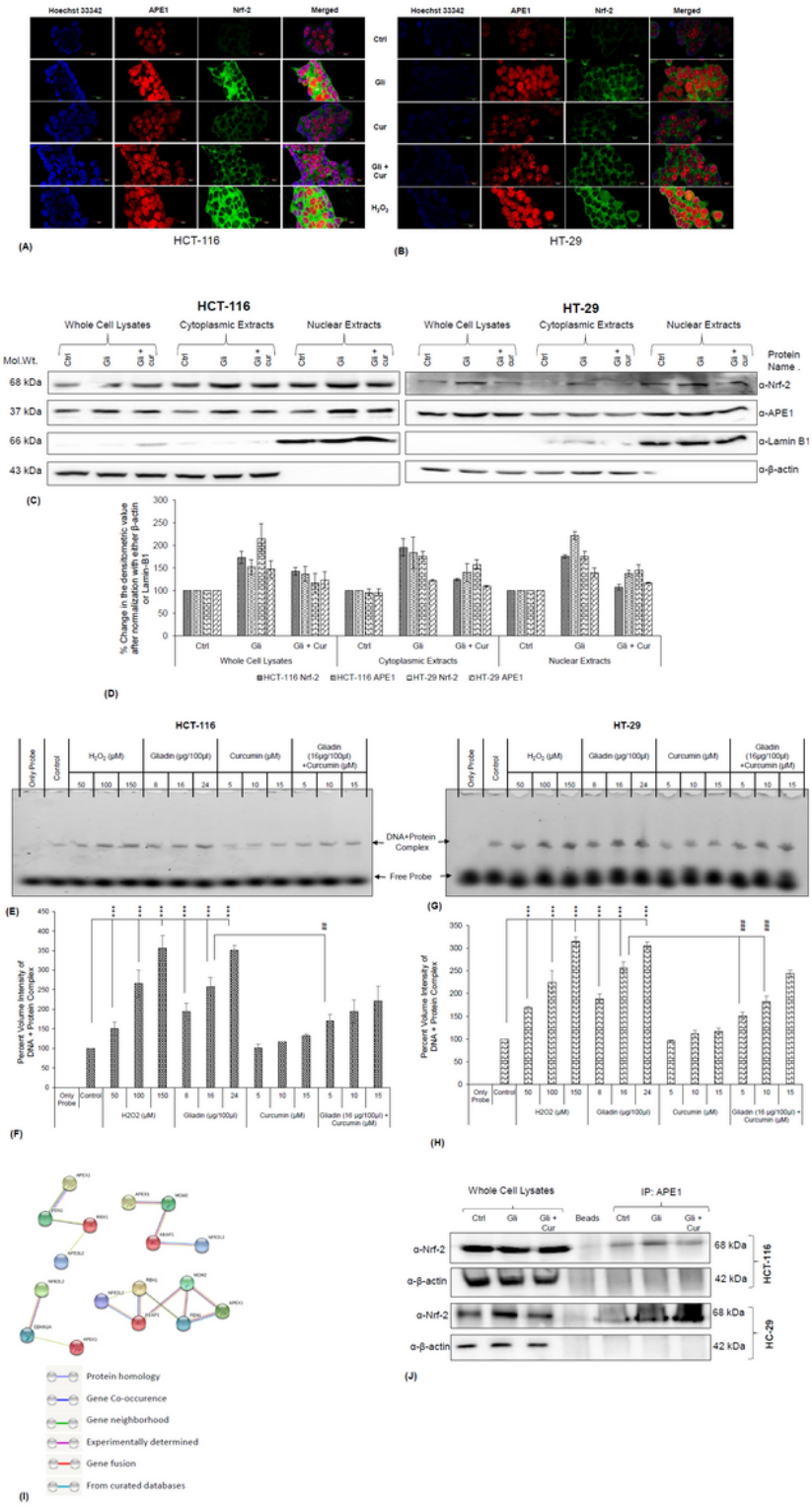

Figure 4

Sub-cellular Localization and Cross-talk of APE1 and Nrf-2: The sub-cellular co-localization of APE1 and Nrf-2 in both cells (HCT-116 & HT-29) after the treatment of Gliadin, Curcumin and their combinations (3 h pretreatment of curcumin) and H2O2 for 24 h was performed. Immunofluorescence based confocal study was performed after staining of these two proteins and counterstaining the nucleus with Hoechst 33342. The representative microscopic images for (A) HCT-116 cells, and (B) HT-29 cells. Western blot based sub-

cellular translocation of APE1 and Nrf-2 was studied using different sub-cellular fractions (whole cell lysates, cytoplasmic extracts and nuclear extracts); (C) the representative Western blot image, and (D) densitometric data after normalization with the respective fraction marker. EMSA based in vitro DNA-protein interaction for the ARE binding protein (Nrf-2) was studied using the nuclear extracts prepared after the different treatments as mentioned above, (E) the representative gel image for HCT-116 cells and (F) densitometric analysis of DNA-protein complex in HCT-116 cells, (G) the representative gel image for HT-29 cells, and (H) densitometric analysis of DNA-protein complex in HT-29 cells. Protein-protein interaction for APE1 and Nrf-2 proteins were studied: (I) STRING (an in silico database based online tool) was used to elucidate the possible interaction between APE1 and Nrf-2. Co-Immunoprecipitation based in vitro interaction between APE1 and Nrf-2 was established in both the cell lines (J) representative images of Co-IP experiments (n=2).

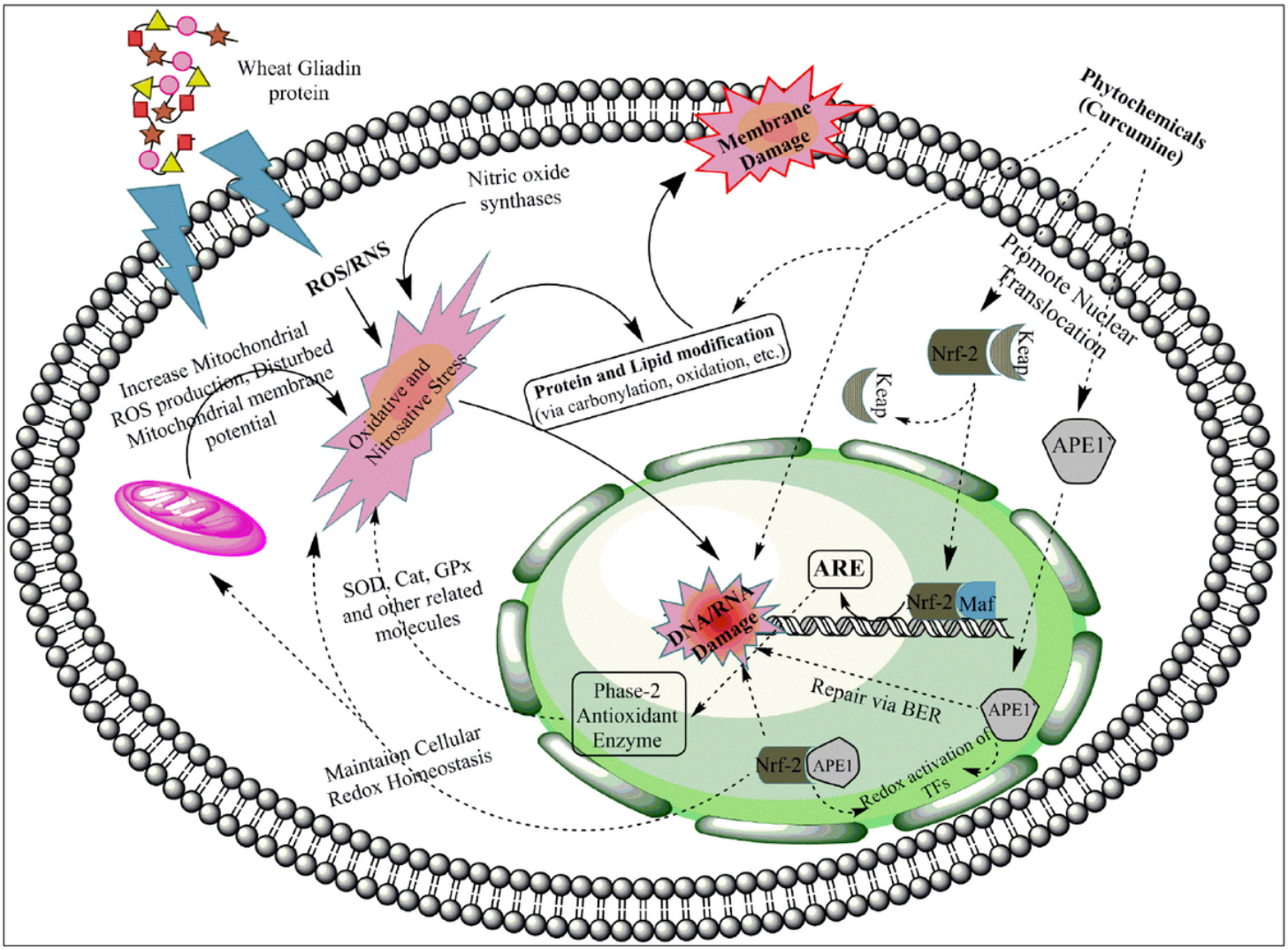

Figure 5

A cartoon model summarizing the role of phytochemical curcumin against gliadin induced oxidative/nitrosative stress-mediated signalling pathways and effect on various cell survival macromolecules.

Supplementary Files

This is a list of supplementary files associated with this preprint. Click to download.

- Supplementaryfigure.pptx